



Published in final edited form as:

Nano Lett. 2009 December ; 9(12): 4370–4375. doi:10.1021/nl902647x.

## Endosomal Leakage and Nuclear Translocation of Multiwalled Carbon Nanotubes: Developing a Model for Cell Uptake

Qingxin Mu<sup>1,2</sup>, Dana L. Broughton<sup>1</sup>, and Bing Yan<sup>1,3,\*</sup>

<sup>1</sup>St. Jude Children's Research Hospital, Memphis, Tennessee 38105

<sup>2</sup>School of Pharmaceutical Sciences, Shandong University, Jinan, China, 250100

<sup>3</sup>School of Chemistry and Chemical Engineering, Shandong University, Jinan, China, 250100

### Abstract

We report our findings on cellular membrane penetration, endocytosis, endosomal leakage and nuclear translocation of multiwalled carbon nanotubes (MWCNTs). Our data is consistent with a working model for MWCNTs' cell uptake and cellular translocations.

Among all nanomaterials, carbon nanotubes (CNTs) possess broadest application potential including electrical circuits,<sup>1</sup> hydrogen storage,<sup>2</sup> drug delivery<sup>3</sup> and tumor imaging.<sup>4</sup> In recent years, the perturbation of CNTs on proteins,<sup>5</sup> cells<sup>6–8</sup> and live animals<sup>9</sup> have also attracted concerns in both public and scientific communities. Because of their tubular structure and extremely high aspect-ratio, CNTs can readily penetrate various biological barriers in mammals,<sup>9</sup> plants,<sup>10</sup> and microorganisms.<sup>11</sup> Furthermore, the large surface area enables CNTs to bind small molecules,<sup>7</sup> proteins<sup>5</sup> and nucleic acids.<sup>12</sup> They may deliver therapeutic payloads or DNA and RNA molecule to cells and interfere with biological processes such as signaling transduction.<sup>6</sup> Therefore, the behavior of CNTs in living cells including cell entrance, subcellular locations and excretion is crucial for their effects on cellular functions. However, the mechanism of cell uptake and cellular fate of CNTs is not fully understood and current descriptions are still controversial especially on cell uptake of CNTs,<sup>13–18</sup> their intracellular translocation, and subcellular localization.<sup>19–23</sup> A popular view is that CNTs are taken up by cells through clathrin-dependent endocytosis.<sup>14</sup> Protein- or DNA-coated SWCNTs were shown to enter cells in an energy-dependent manner. Although majority of published data agree with the endocytosis model, the energy-independent cell uptake was also reported.<sup>15</sup> The authors argued that the different mechanisms of cell uptake could be due to the different surface characteristics of CNTs. Another controversy is on subcellular locations of CNTs. Reports described that CNTs go into cells without entering nucleus<sup>21, 24, 25</sup> while other reports found that SWCNT entered cell nucleus<sup>17, 19, 22, 23</sup> and this entrance might be reversible.<sup>22</sup> However, there is no knowledge whether MWCNTs can enter cell nucleus. Furthermore, it is still not clear how CNTs can enter cytoplasm to interact with proteins, enzymes, and deliver therapeutic agents.

Understanding of mechanisms of cell entrance, intracellular translocation, subcellular locations, and the excretion of CNTs is of utmost importance in order to elucidate CNTs' possible hazards and their potentials for drug/gene delivery. Herein, we report our

\*Corresponding author: To whom correspondence should be addressed. Phone: +9014952797. Fax: +9014955715. bing.yan@stjude.org. Supporting Information Available. Details of the experimental procedure, FT-IR characterization of MWCNTs, identification of MWCNT bound proteins, cell growth measurement, and additional TEM images are available. This materials is available free of charge via the Internet at <http://pubs.acs.org>.

ultrastructural observations of cell uptakes of CNTs into human embryonic kidney epithelial cells (HEK293). On the basis of our experimental observations and inference from previous reports, a plausible model for MWCNTs' cellular circulation path is proposed. Single MWCNTs enter cells through direct penetration while MWCNT bundles through endocytosis. MWCNT bundles in endosomes may release single nanotubes that then penetrate endosome membrane and escape into cytoplasm. Short MWCNTs can also enter cell nucleus. All classes of MWCNTs are recruited into lysosome for excretion. This model helps unify previous controversies and provides novel insights into MWCNTs' cellular circulations.

Endocytosis is energy-dependent and characterized by its temperature dependence.<sup>26</sup> To compare the effect of surface charge on cell uptake, we synthesized both carboxylated (MWCNT-COOH) and aminated (MWCNT-NH<sub>2</sub>) CNTs (Supporting Information and Figure S1). Morphology of MWCNT-COOH and MWCNT-NH<sub>2</sub> was observed by TEM (Figure 1A&B). The diameter of MWCNTs is around 20–30 nm. Since sonication may cut nanotubes short, the length distributions were determined. The average length of both MWCNTs was ~1000 nm (Figure 1C&D). The temperature-dependence of fluorescent MWCNTs was first measured by flow cytometry and epifluorescence microscopy. MWCNT-COOH and MWCNT-NH<sub>2</sub> were first coated with FITC-BSA through strong adsorption mediated by  $\pi$ - $\pi$  stacking and electrostatic interactions between MWCNTs and proteins.<sup>5, 6</sup> Free proteins were removed by five washing/centrifuging cycles. CNTs were then incubated with HEK293 cells for one hour in both 37°C and 4°C. Both flow cytometry and fluorescence microscopic imaging showed that MWCNTs with opposite surface charges were taken up by cells in a similar temperature-dependent manner (Figure 2) indicating both MWCNTs could enter cell through endocytosis.

Since the temperature-dependent uptake of positively charged MWCNT-NH<sub>2</sub> was similar to negatively charged MWCNT-COOH in above experiments, we speculated that the protein coating and the effects on surface potential might be responsible for the observed similarity in endocytotic cell uptake of two MWCNTs. The opposite surface charges on these two MWCNTs in H<sub>2</sub>O were reflected in Zeta potentials of MWCNT-COOH (−57 mV) and MWCNT-NH<sub>2</sub> (+26 mV). Surface charges of MWCNTs were overwhelmingly modified in cell culture medium containing serum proteins. Zeta potential of MWCNT-COOH and MWCNT-NH<sub>2</sub> in cell culture medium was changed to −48 mV and −35 mV due to protein binding (Supporting Information and Table S1). As proteins abundantly exist in biological fluids, protein bindings in general may significantly change CNTs' surface characteristics *in vivo*. Proteins bound to both MWCNTs were identified by LC-MS/MS analysis showing that 55 most abundant proteins bound to MWCNT-COOH and 37 to MWCNT-NH<sub>2</sub> (Supporting Information and Table S1). Therefore, heavy protein coating on both MWCNTs made MWCNTs with opposite charges similar nanostructures in term of surface charges. This similarity may directly impact their abilities to interact with cells.

Flow cytometry and fluorescence microscope only detect gross fluorescence that emit from cells, highly dispersed CNTs, such as single nanotubes, might not be detectable by either technique. The cell uptake of single nanotubes must be investigated by other methods, such as TEM. TEM was performed on cells incubated with MWCNTs for one hour and 48 hrs. About 20 images were acquired for each sample and the representative images are shown in Figure 3 and 4 and Supporting Information (Fig. S3 and S4). The entrance of single MWCNTs was repeatedly observed by TEM. For example, figure 3A shows that a single MWCNT-COOH is penetrating plasma membrane. Our data suggest that direct penetration can be designated as one of the routes to deliver MWCNTs into cytoplasm. In contrast to single MWCNTs, bundled MWCNT-COOH tended to enter cells through endocytosis and, in the beginning, trapped in intracellular endosomes (Figure 3B) consistent with result from flow cytometry and fluorescence microscopy. MWCNT-COOH bundles within endosomes then released single

MWCNTs that penetrated the endosomal membrane and escaped into cytoplasm (Figure 3C&D, SI Figure S3) providing another route for MWCNTs to enter cytoplasm. Due to the direct penetration into cells and escaping from endosomes, single MWCNTs were frequently observed in the cytoplasm (Figure 3D, G & 4C, E, and Figure S3 in Supporting Information). At 48 hours, cytoplasmic MWCNT and endosomal escape were also observed (Figure 3F & G). At this time point, much more MWCNT-COOHs were recruited into lysosomes (Figure 3E and H). The plasma and endosomal membrane penetration mode of cell entrance based on TEM complements the endocytosis model observed previously by other researchers<sup>14</sup> and our data in previous sections.

Similar to MWCNT-COOH, MWCNT-NH<sub>2</sub>s also enter cells through endocytosis and direct penetration. The MWCNT-NH<sub>2</sub> bundles in endosomes also released single MWCNTs that might penetrate endosomal membrane and enter the cytoplasm (Figure 4A&B). The cytoplasmic accumulation of single MWCNT-NH<sub>2</sub>s (Figure 4C & E, SI Figure S4) was also results of both direct permeation and endosomal escape of single MWCNT-NH<sub>2</sub> (Figure 4B). The endosomal escape of MWCNT-NH<sub>2</sub> indicated that the strong membrane insertion ability of MWCNTs did not depend on surface charge of MWCNTs after protein coating modifications in biological fluid. The fusion of endosome-like vesicles with lysosomes was observed (Figure 4D) and the accumulation of MWCNTs in lysosome was observed (Figure 4F). As a sorting station, substances in endosome are often transported into various compartments such as Golgi apparatus, endoplasmic reticulum (ER) or lysosome<sup>27</sup>. Through carefully examination, we could not find nanotubes in Golgi apparatus or ER in our experiments. Our observations indicated that recruitment of MWCNT bundles into lysosomes was the most possible route for their cellular fate.

The accumulation of cytoplasmic MWCNTs increased their chance to enter nucleus. Cell nucleus consists of double layered membrane envelop that separate its contents from the cytoplasm. It's impermeable to most molecules unless those that are able to penetrate through nuclear pores.<sup>28</sup> TEM examinations identified a MWCNT-NH<sub>2</sub> (Figure 4G and H) in the nucleus. This result documented the first direct observation of MWCNT located in a cell nucleus.

Cell uptake of MWCNTs, whether through endocytosis or direct penetration, does not depend on their surface charges when they are modified by protein coating. The effect of the dimension or length of MWCNTs on cellular uptake still needs to address. We next measured the length of individual nanotubes that were taken up by cells after 1 hour. About 100 nanotubes with proper orientations were measured and the histograms were generated (Figure 5). The histograms show that the average lengths of MWCNT-COOH and MWCNT-NH<sub>2</sub> in cells are around 250 nm and 175 nm, respectively while the average length of MWCNTs is ~1000 nm when they first added to cell culture. Since only tubes lying in the cell section plane could be measured for their length, we examined ~20 TEM micrographs from random transverse sections of cells and only counted those tubes with proper orientations. The nanotube length distribution therefore represents the best approximation on the basis of our TEM results. This data demonstrate that shorter MWCNTs have stronger propensity to penetrate plasma membranes. This finding offers us an essential strategy for targeting cytoplasm and nucleus using CNTs as delivery vehicles. Although MWCNTs occupied most subcellular organelles, no cell death was observed except some cell growth inhibition for both MWCNTs (Supporting Information, Figure S2).

Recently processes for cell uptake were described as clathrin-dependent endocytosis<sup>14</sup> and endocytosis-independent cell uptake.<sup>15</sup> Subcellular locations of CNTs were also pinpointed in scattered studies.<sup>18, 20, 22, 23, 25</sup> CNTs were found in cytoplasm, in endosomes, and lysosomes. Only SWCNTs were found in cell nucleus. These phenomena were separately reported and

currently there is no model that describes the cellular circulation of CNTs, from cell entrance to excretion. Previous reports and our own experimental results are consistent with a working model for the cell uptake of CNTs (Figure 6). In this model, CNTs are divided into two classes, clusters and singles. CNT clusters are taken up by cells through energy-dependent endocytosis process. The CNT bundles then release single nanotubes that escape endosomes by penetrating endosome membrane and entering the cytoplasm. Alternatively, the highly dispersed single CNTs cross cell membrane and enter cells directly by penetrating cellular membranes. All CNTs are recruited into lysosomes for excretion. Cytoplasmic CNTs can also enter nucleus suggesting the strong ability of CNT to cross several biological membrane barriers.

In summary, we observed the size dependent and direct membrane penetration by both negatively and positively charged single MWCNTs, endocytosis of bundled MWCNTs, the endosomal leakage of single MWCNTs from bundles, and the nuclear translocation of MWCNT. Based on our experimental observations and previous reports, we proposed a working model that describes our current understanding of CNTs' cell uptake. The model will have major impacts on both drug delivery and toxicity research of CNTs. For example, all cellular CNTs may be exposed to cytoplasm so that the unexpected interactions with cellular functional molecules are likely to occur. Therefore, a better understanding of CNTs' cellular behavior provides both opportunities and challenges on the way to the development of nanomedicine.

## Supplementary Material

Refer to Web version on PubMed Central for supplementary material.

## Acknowledgments

We thank Ms. Linda Mann (Cell and tissue imaging, St. Jude Children's Research Hospital) for the technical assistance on TEM and Hartwell Center for Bioinformatics & Biotechnology at St. Jude Children's Research Hospital for proteomics analysis. This work was supported by National Cancer Institute (P30CA027165), the American Lebanese Syrian Associated Charities (ALSAC) and St. Jude Children's Research Hospital.

## References

1. Collins PC, Arnold MS, Avouris P. *Science* 2001;292:706–709. [PubMed: 11326094]
2. Dillon AC, Jones KM, Bekkedahl TA, Kiang CH, Bethune DS, Heben MJ. *Nature* 1997;386:377–379.
3. Bianco A, Kostarelos K, Prato M. *Curr. Opin. Chem. Biol* 2005;9:674–679. [PubMed: 16233988]
4. Zavaleta C, de la Zerde A, Liu Z, Keren S, Cheng Z, Schipper M, Chen X, Dai H, Gambhir SS. *Nano Lett* 2008;8:2800–2805. [PubMed: 18683988]
5. Mu Q, Liu W, Xing Y, Zhou H, Li Z, Zhang Y, Ji L, Wang F, Si Z, Zhang B, Yan B. *J. Phys. Chem. C* 2008;112:3300–3307.
6. Mu Q, Du G, Chen T, Zhang B, Yan B. *ACS Nano* 2009;3:1139–1144. [PubMed: 19402638]
7. Zhou HY, Mu QX, Gao NN, Liu AF, Xing YH, Gao SL, Zhang Q, Qu GB, Chen YY, Liu G, Zhang B, Yan B. *Nano Lett* 2008;8:859–865. [PubMed: 18288815]
8. Wick P, Manser P, Limbach LK, Dettlaff-Weglikowska U, Krumeich F, Roth S, Stark WJ, Bruinink A. *Toxicol. Lett* 2007;168:121–131. [PubMed: 17169512]
9. Qu GB, Bai YH, Zhang Y, Jia Q, Zhang WD, Yan B. *Carbon* 2009;47:2060–2069.
10. Liu QL, Chen B, Wang QL, Shi XL, Xiao ZY, Lin JX, Fang XH. *Nano Lett* 2009;9:1007–1010. [PubMed: 19191500]
11. Kang S, Herzberg M, Rodrigues DF, Elimelech M. *Langmuir* 2008;24:6409–6413. [PubMed: 18512881]
12. Li X, Peng YH, Ren JS, Qu XG. *Proc. Natl. Acad. Sci. U. S. A* 2006;103:19658–19663. [PubMed: 17167055]

13. Chin SF, Baughman RH, Dalton AB, Dieckmann GR, Draper RK, Mikoryak C, Musselman IH, Poenitzsch VZ, Xie H, Pantano P. *Exp. Biol. Med* 2007;232:1236–1244.
14. Kam NWS, Liu ZA, Dai HJ. *Angew. Chem.-Int. Edit* 2006;45:577–581.
15. Kostarelos K, Lacerda L, Pastorin G, Wu W, Wieckowski S, Luangsivilay J, Godefroy S, Pantarotto D, Briand JP, Muller S, Prato M, Bianco A. *Nat. Nanotechnol* 2007;2:108–113. [PubMed: 18654229]
16. Lacerda L, Raffa S, Prato M, Bianco A, Kostarelos K. *Nano Today* 2007;2:38–43.
17. Pantarotto D, Briand JP, Prato M, Bianco A. *Chem. Commun* 2004:16–17.
18. Zhu Y, Li WX, Li QN, Li YG, Li YF, Zhang XY, Huang Q. *Carbon* 2009;47:1351–1358.
19. Mooney E, Dockery P, Greiser U, Murphy M, Barron V. *Nano Lett* 2008;8:2137–2143. [PubMed: 18624387]
20. Porter AE, Gass M, Muller K, Skepper JN, Midgley PA, Welland M. *Nat. Nanotechnol* 2007;2:713–717. [PubMed: 18654411]
21. Lacerda L, Pastorin G, Gathercole D, Buddle J, Prato M, Bianco A, Kostarelos K. *Adv. Mater* 2007;19:1480–1484.
22. Cheng JP, Fernando KAS, Veca LM, Sun YP, Lamond AI, Lam YW, Cheng SH. *ACS Nano* 2008;2:2085–2094. [PubMed: 19206455]
23. Porter AE, Gass M, Bendall JS, Muller K, Goode A, Skepper JN, Midgley PA, Welland M. *ACS Nano* 2009;3:1485. [PubMed: 19459622]
24. Zhang DW, Yi CQ, Zhang JC, Chen Y, Yao XS, Yang MS. *Nanotechnology* 2007;18:9.
25. Kang B, Yu DC, Chang SQ, Chen D, Dai YD, Ding YT. *Nanotechnology* 2008;19:8.
26. Weigel PH, Oka JA. *J. Biol. Chem* 1981;256:2615–2617. [PubMed: 6259136]
27. Mellman I. *Ann. Rev. Cell Dev. Biol* 1996;12:575–625. [PubMed: 8970738]
28. Terry LJ, Shows EB, Wenthe SR. *Science* 2007;318:1412–1416. [PubMed: 18048681]

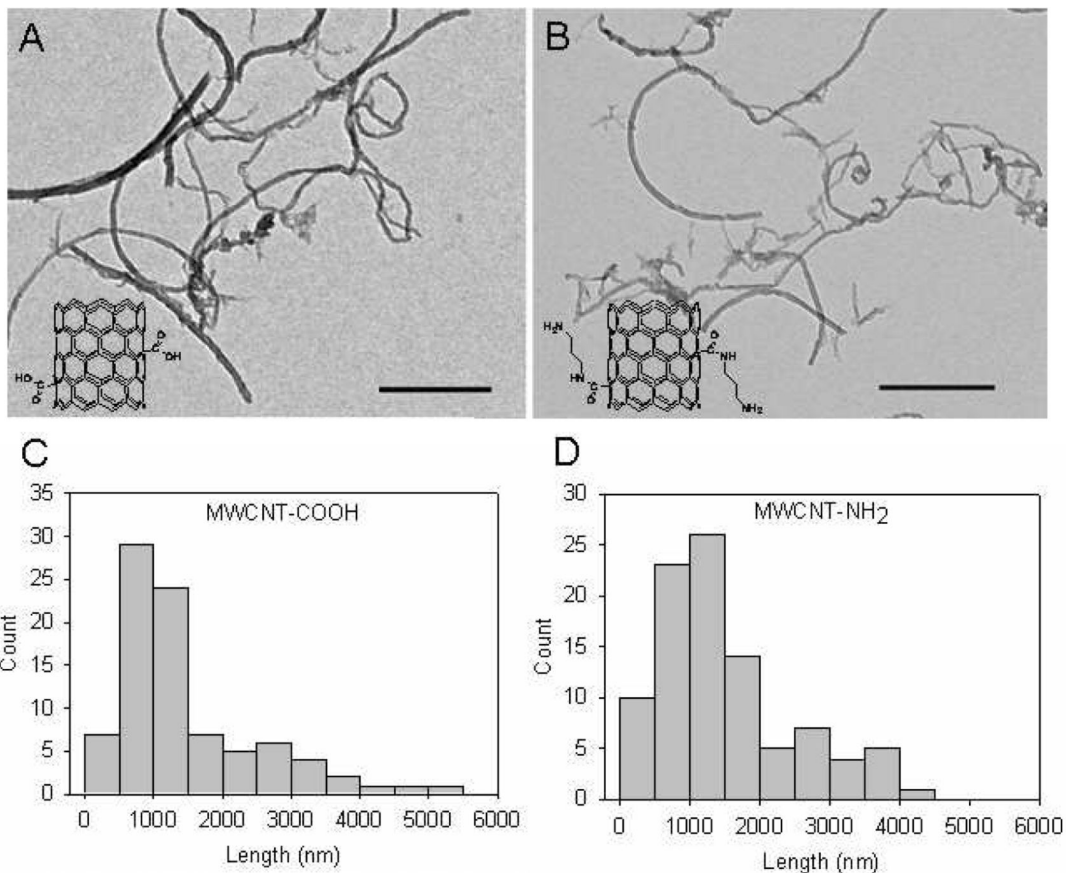


**Figure 1.** Characterization of MWCNT-COOH and MWCNT-NH<sub>2</sub> by TEM. Upper panel: TEM images of MWCNT-COOH (A) and MWCNT-NH<sub>2</sub> (B). Scale bars indicate 500 nm. Insets: chemical structures of MWCNTs. Lower panels: length distributions of MWCNT-COOH (C) and MWCNT-NH<sub>2</sub> (D) in H<sub>2</sub>O after 5 minutes sonication. Each histogram was generated based on counting ~100 nanotubes.



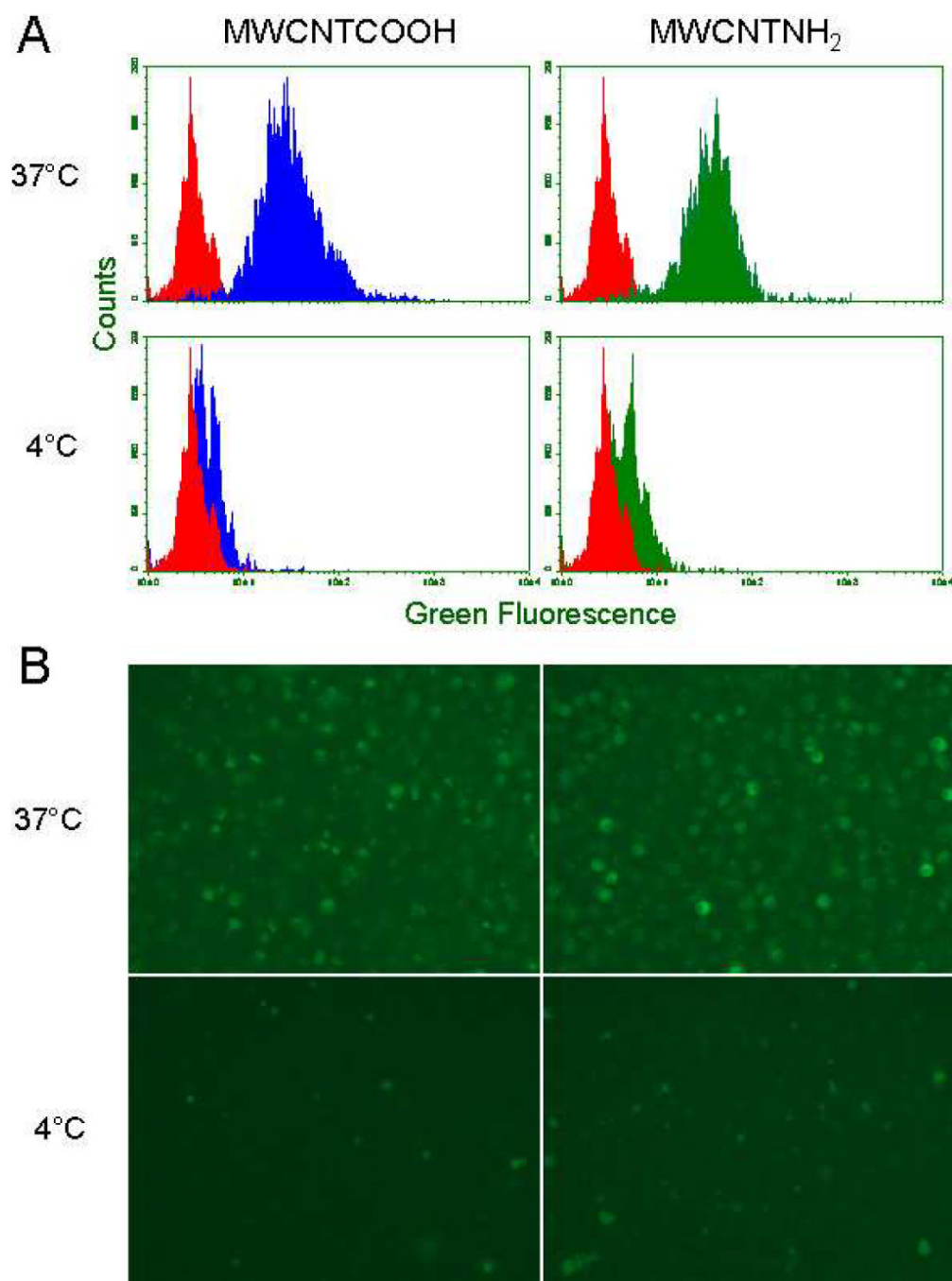
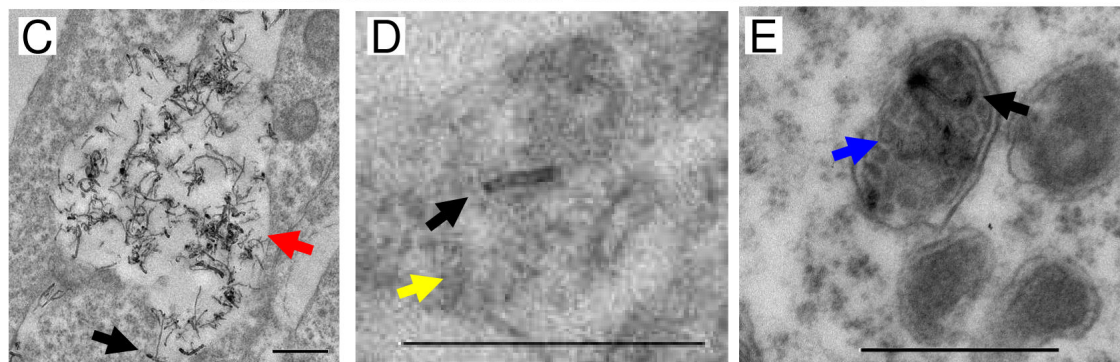
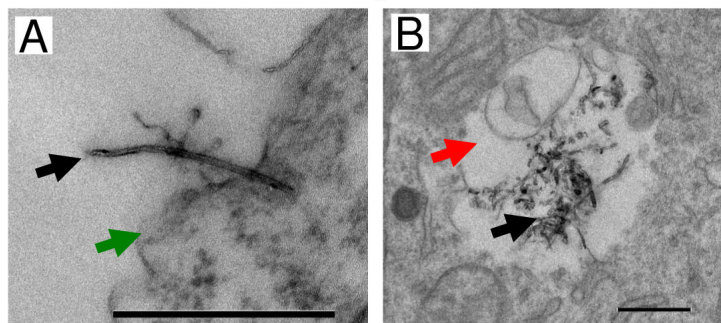
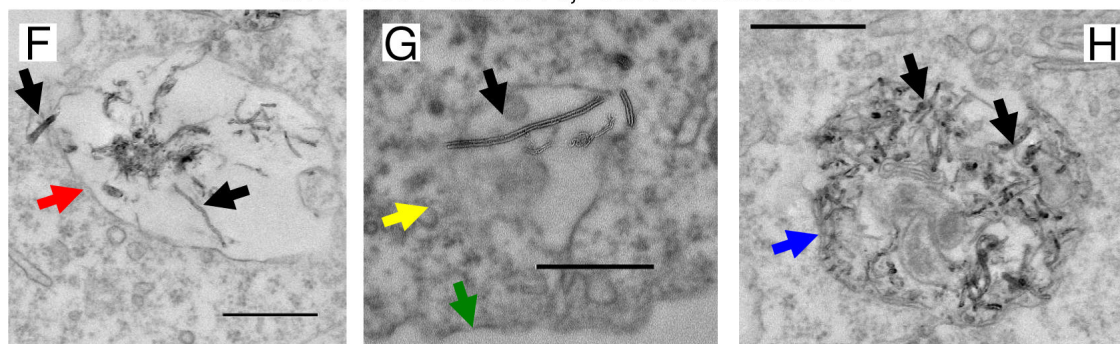


**Figure 2.** Energy-dependent cell uptake of MWCNTs. A. Flow cytometry analysis; B, epifluorescence images. HEK293 cells were incubated with FITC-BSA labeled MWCNT-COOH and MWCNT-NH<sub>2</sub> for 1 hour at 37°C and 4°C, respectively. Cells were detached and aspirated prior to flow cytometry or imaging analysis.

## MWCNT-COOH, 1h incubation



## MWCNT-COOH, 48h incubation



 Plasma membrane  
 Cytoplasm

 Endosome  
 Lysosome

 MWCNTs

**Figure 3.**

TEM characterization of cell uptake of MWCNT-COOHs and their cellular localizations in HEK293 cells. Cells were incubated with nanotubes (100  $\mu\text{g}/\text{mL}$ ) at 37°C for 1 hour and 48 hours, respectively. The cells were then fixed, embedded and sectioned followed by imaging analysis. Arrows indicate organelles or MWCNT-COOHs, green: plasma membrane; red: endosome; yellow: cytoplasm; blue: lysosome; black: MWCNT-COOH. All scale bars represent 500 nm.



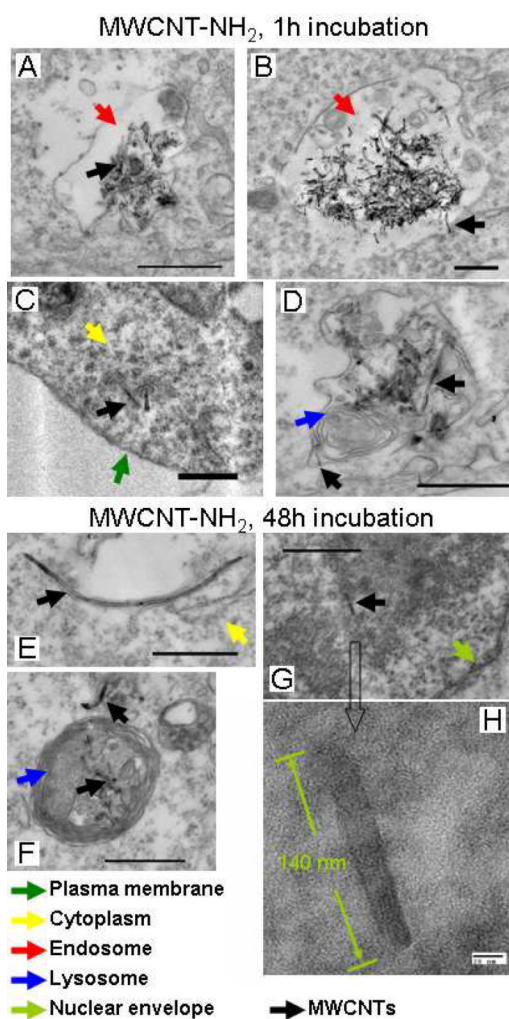


**Figure 4.** TEM characterization of cell uptake of MWCNT-NH<sub>2</sub>s and their cellular localizations in HEK293 cells. Cells were incubated with nanotubes (100  $\mu\text{g}/\text{mL}$ ) at 37°C for 1 hour and 48 hours, respectively. The cells were then fixed, embedded and sectioned followed by imaging analysis. Arrows indicate organelles or MWCNT-NH<sub>2</sub>s, green: plasma membrane; red: endosome; yellow: cytoplasm; blue: lysosome; black: MWCNT-NH<sub>2</sub>. All scale bars represent 500 nm.

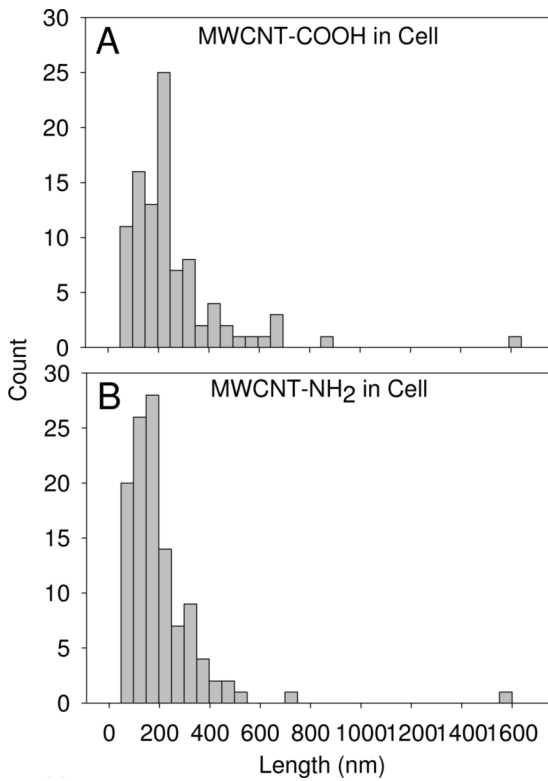


**Figure 5.** Length distributions of MWCNT-COOH (A) and MWCNT-NH<sub>2</sub> (B) inside cells after 1 hour incubation with MWCNTs at 37°C. Each histogram was generated based on counting 100 individual nanotubes with proper orientations.

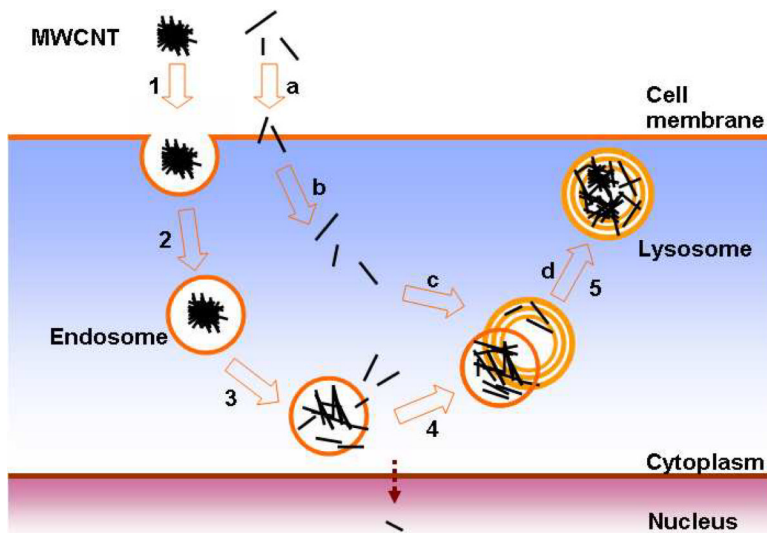


**Figure 6.** A working model for cell uptake of MWCNTs. Numbers (1–5) and letters (a–d) indicate different steps in two possible cellular translocation pathways of MWCNTs. The bundled MWCNTs bind to cell membranes (1), and are subsequently internalized into cells (2) inside endosomes. In the endosomes, bundles release single MWCNTs that penetrate endosomal membranes and enter cytoplasm (3). Both residual bundled MWCNTs in endosomes and free MWCNTs in the cytoplasm are recruited into lysosomes for excretion (4 and 5). Single MWCNTs enter cells through direct membrane penetration (a) to enter cytoplasm (b). They are recruited into lysosomes for excretion (c and d). Short MWCNTs are also able to enter nucleus.